Enthalpy Relaxation of Photopolymerized Thiol−Ene Networks: Structural Effects

Junghwan Shin, Sergei Nazarenko, and Charles E. Hoyle*

School of Polymer and High Performance Materials, University of Southern Mississippi, Hattiesburg, Mississippi 39406

Received April 18, 2008; Revised Manuscript Received July 3, 2008

ABSTRACT: Physical aging behavior of photopolymerized thiol−ene networks was investigated by measuring the extent of enthalpy relaxation in terms of network density and molecular structure. The homogeneous network structure of the thiol−enes, having narrow glass transition temperature ranges, showed characteristic temperature and time dependency relationships for enthalpy relaxation. All thiol−ene films annealed at different temperatures (T_a) for 1 h according to the isochronal method showed maximum enthalpy relaxation peaks at approximately T_g − 10 °C by DSC. The extent of enthalpy relaxation as a function of annealing time (t_a) was obtained by the isothermal aging method. Correlations between the extent of enthalpy relaxation and the heat capacity difference at T_g were made and related to thiol−ene chemical group rigidity and network linking density. Pendulum hardness values for a selected thiol−ene film showed a clear change in hardness upon aging, indicating sub-T_g mechanical relaxation, consistent with the related enthalpy relaxation process.

Introduction

Polymer sub-T_g aging behavior is related to the molecular structure and chemical environment which control chain mobility and conformational states. Hence, the chemical structure of linear, cross-linked, and network polymers can potentially have a profound effect on the extent of enthalpy relaxation. As examples of linear polymers, poly(vinyl acetate),[1] polycarbonate,[2] poly(methyl methacrylate),[3,4] polystyrene,[5−7] and phenolphthalein poly(ether sulfone)[8] have been investigated in terms of the effect of molecular weight, chain conformation, and entanglement on enthalpy relaxation. The roles of hydrogen bonding and bulky side chains of linear polymers have also been reported.[9] Since physical aging is directly related to segmental relaxation, the effect of chain mobility, cross-link density, and the molecular weight between cross-links is important.[10] Accordingly, the segmental relaxation behavior of cross-linked poly(ethylene oxide) copolymers showed an increase in broadening of the segmental relaxation distribution.[11] Attention has also been paid to epoxy systems, which are well-known to form polymer network structures that undergo physical aging.[12−16] Since epoxy networks are chemically complex due to significant effects from hydrogen bonding, difficulty in controlling the extent of reaction, and chemical side reactions, correlation of structure−property relationships can be challenging.

Thiol−enes are important in the fields of coatings, adhesives, and energy damping because of important attributes such as insensitivity to oxygen during photopolymerization, high conversion, and low shrinkage.[17−21] Unlike other photoinitiated polymerization processes, thiol−enes follow a free-radical step-growth reaction mechanism that proceeds by a two-step propagation process.[17] Thiol−ene mixtures still exist as low molecular weight prepolymers until the gel point, resulting in a combination of low stress-induced shrinkage and high conversion. Because of essentially quantitative conversions and a free-radical step-growth process, photopolymerized thiol−ene films are highly uniform with dense network structures as depicted pictorially in Chart 1 for a generic trifunctional thiol and trifunctional ene.

Compared to conventional linear or cross-linked polymers, thiol−ene-based networks have a highly uniform dense structure and inherently narrow glass transition.[17−21] This suggests that thiol−ene networks might be very sensitive to annealing temperature and time, resulting in a large amount of enthalpy or volume relaxation in a short period of time under specific physical aging conditions (temperature, pressure). Since thiol−ene networks have significance as coatings, energy-absorbing materials, and optical components, any changes that may occur due to sub-T_g relaxation process are essential to identify and characterize. As already described, the near-perfect network structure of photopolymerized thiol−ene systems which proceed to quantitative conversion with no side reactions, except for a small amount of radical coupling, presents a unique opportunity to evaluate enthalpy relaxation fundamentals in network systems. Accordingly, in the research described herein, the aging of photopolymerized thiol−ene networks was evaluated by measuring the extent of enthalpy relaxation in terms of network density and chemical structural effects. The roles of chemical structural features such as rigidity and network density are established.

Chart 1. Uniform Network Structure of Generic Trithiol−Triene Network

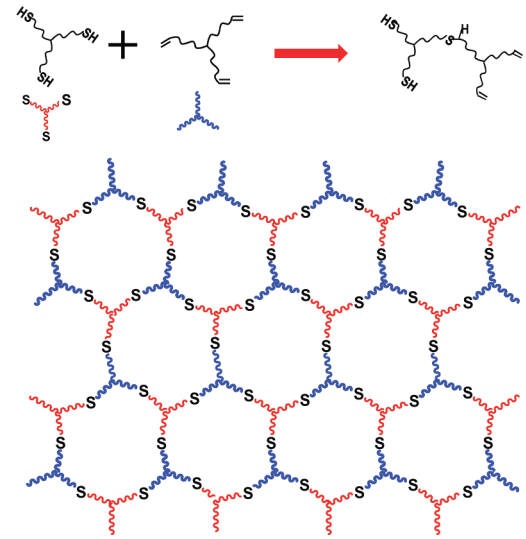

* Corresponding author. E-mail: charles.hoyle@usm.edu.

10.1021/ma800863n CCC: $40.75
Published on Web 08/21/2008

Chart 2. Structure of Thiol and Ene Monomers

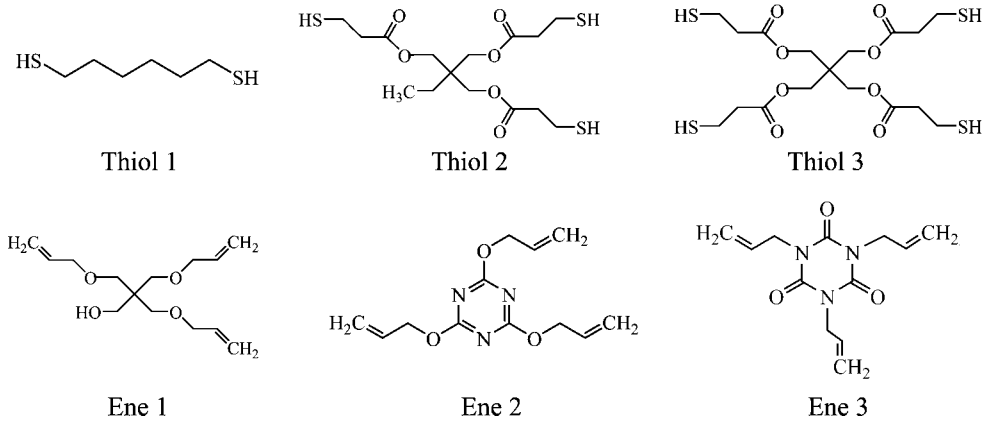

Experimental Section

1,6-Hexanedithiol (Thiol 1), 2,4,6-triallyloxy-1,3,5-triazine (Ene 2), and 1,3,5-triallyl-1,3,5-triazine-2,4,6(1*H*,3*H*,5*H*)-trione (Ene 3) were purchased from Aldrich, and the other thiols (triethrylolpropane tris(3-mercaptopropionate) (Thiol 2) and pentaerythritol tetrakis(3-mercaptopropionate) (Thiol 3)) and ene monomer (allylpentaerythritol (Ene 1)) were obtained from Bruno Bock Thio-Chemicals-S and Perstorp Specialty Chemicals, respectively. All thiol and ene monomers used in the investigation are shown in Chart 2. The photoinitiator, 2,2-dimethoxy-2-phenylacetophenone (DMPA), was supplied by Ciba Specialty Chemicals. All materials were used as received.

The photoinitiator (DMPA, 1 wt %) was dissolved in the thiol and ene mixtures by sonication for 10−20 min. All thiol−ene films were cast on glass plates (200 μm draw-down bar) and cured by passing 10 times on a Fusion UV curing line system equipped with a D bulb (400 W/cm^2 with belt speed of 10 feet/min and 3.1 W/cm^2 irradiance). Surface temperature of films during curing reached 70−80 °C, and all samples were postcured at 80 °C for 24 h to complete the reaction and remove any chemical conversion effect on enthalpy relaxation.

Kinetic profiles of thiol−ene photopolymerization were obtained using real-time infrared (RTIR) spectroscopy. Infrared spectra were recorded on a modified Bruker 88 Fourier transform infrared spectrometer designed to allow light to impinge on a horizontal sample with a fiber-optic cable as a function of the irradiation time. An Oriel 200 W, high pressure mercury−xenon lamp equipped with a light pipe was directed to a 20 μm sample between two salt plates. The light impinging on the sample had an irradiance of 7.8 mW/cm^2 at 365 nm. The temperature was isothermally controlled at 80 °C to provide a similar temperature environment to that experienced by samples cured using the Fusion lamp. The conversion rates were monitored at 3080 cm^{-1} for enes and 2570 cm^{-1} for thiols.

A TA Q1000 DSC with RCS 90 (refrigerated cooling system) was used to measure thermal behavior of thiol−ene networks before and after sub-T_g annealing. A RCS 90 cooling head mounted on the DSC Q1000 furnace encased the DSC cell, preventing frost building up during operation. Three calibration steps for the TA Q1000 were performed periodically. First, the T_{zero} calibration, both without and with standard material (sapphire), was conducted from −90 to 400 °C to compensate for thermal lag between samples and temperature control sensors. Through the enthalpy constant calibration comparing the heat of fusion of a standard material (indium, 28.58 J/g) with the measured value, the cell constant was determined by the ratio of these two values (1 ± 0.05). Temperature calibration was performed by comparing the known melting point of indium (156.6 °C) with the recorded value during a heating scan. All experiments were carried out under nitrogen with a flow rate of 50 mL/min. Sample weights were 8.0 ± 1.0 mg to ensure sufficient sensitivity for heat capacity measurements. DSC scans were conducted over the temperature range from T_g − 50 °C to T_g + 50 °C using 10 °C/min heating (q_h) and cooling (q_c) rates. It was assumed that initializing the thiol−ene network before each aging process at T_g + 50 °C was sufficient to erase the internal stress from the photopolymerization and/or any previous physical aging history. Enthalpy relaxation behavior of the networks was studied by two different methods. First, thiol−ene film samples were annealed directly in the DSC at various temperatures (T_a was varied every 5 °C from T_g + 10 to T_g − 50 °C) for 60 min (t_a) in order to obtain information on the temperature dependency of the enthalpy relaxation rate (isochronal method, Figure 1a). Second, the enthalpy relaxation was studied as a function of annealing time (up to 24 h) at the temperature where the enthalpy relaxation rate was found to be the fastest by the isochronal method (isothermal method, Figure 1b). The schematic diagrams of the DSC measurement procedures for both methods are shown in Figure 2. Each sample was measured twice. In the isochronal case, samples were measured first sequentially from $T_{a,1}$ to $T_{a,7}$ and then from $T_{a,7}$ to $T_{a,1}$ (Figure 2a). In the isothermal process, samples were processed sequentially from $t_{a,1}$ to $t_{a,4}$ and then from $t_{a,4}$ to $t_{a,1}$ (Figure 2b). Identical results were obtained, thus eliminating the possibility that chemical changes occurred during heating/cooling/annealing cycles. Agreement between the two sets of results illustrates the absence of significant contributions from instrument drift.

The enthalpy relaxation during the sub-T_g aging was calculated from the difference thermograms generated by subtracting the reference DSC curve obtained without annealing from the DSC curve after the sub-T_g annealing process based on the equation

$$\Delta H_r(T_a, t_a) = \int_{T_g-50^\circ C}^{T_g+50^\circ C} C_p(T_a, t_a)\, dT - \int_{T_g-50^\circ C}^{T_g+50^\circ C} C_p(T_a, 0)\, dT \quad (1)$$

where $C_p(T_a,t_a)$ and $C_p(T_a,0)$ represent specific heat capacities for samples annealed at T_a for $t = t_a$ and unannealed samples, respectively.[23−25]

A BYK Gardner pendulum hardness tester was used to determine Persoz pendulum hardness of the annealed networks. The hardness was determined for the Thiol 3 + Ene 3 system which exhibited a

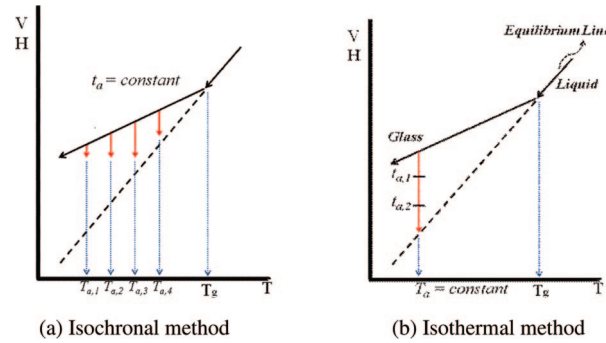

Figure 1. Schematic representation of two annealing methods.[22]

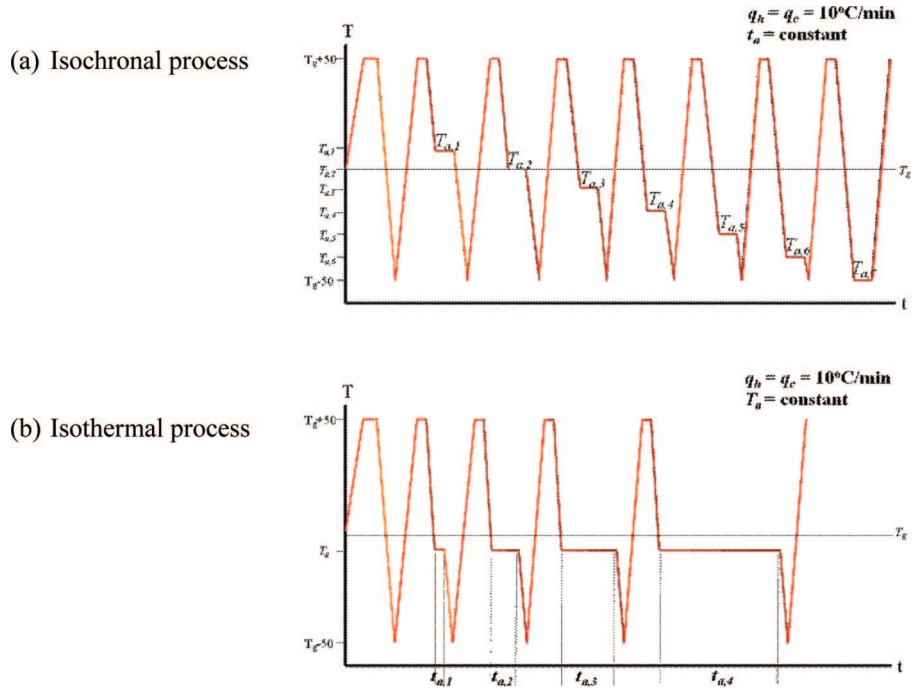

Figure 2. Schematic diagrams of isochronal and isothermal physical aging processes.

glass transition temperature above room temperature. The hardness was measured after annealing the network film at T_g − 10 °C (43 °C) as a function of annealing time to investigate the effect of physical aging on hardness. Measurements were conducted at room temperature on network films coated onto glass substrates. Three different samples, prepared and annealed using the same conditions, were used, and the hardness was measured at least 10 times for each sample. The results of these measurements were averaged.

Results and Discussion

A series of thiols and enes (Chart 2) with significant variation in functionality (2 to 4) and structural rigidity were chosen to answer the basic questions of how network density and the rigidity of chemical groups influence enthalpy relaxation in networks. Although discussed in the Introduction, we reiterate that photopolymerized thiol−ene networks are characterized by essentially quantitative conversions of the monomer components with little or no residual chemical groups that may further react upon thermal cycling or aging. Since they are mechanically and physically highly uniform polymer networks,[17−19] the photocured thiol−ene films made from the components in Chart 2 are ideal for determination of how basic features such as rigidity and network density can influence sub-T_g aging.

DSC heating scans of all nine photopolymerized thiol−ene network samples, after they were heated above their corresponding glass transitions (T_g + 50 °C) and cooled at 10 °C/min down to well below T_g (T_g − 50 °C), are shown in Figure 3. This series of thiol−ene films exhibited a fairly large range of glass transition temperatures, the lowest at about −40 °C for Thiol 1 + Ene 1 and the highest at about +50 °C for the Thiol 3 + Ene 3 system. All of the photopolymerized thiol + ene networks had fairly narrow glass transitions ranges of about 15−20 °C due to the uniform network structure of thiol−enes, as already discussed. To illustrate that essentially quantitative conversion was obtained for each of the samples, in Figure 4, the polymerization kinetic profile for the thiol−ene (Thiol 3 + Ene 3) with the highest T_g was recorded (see Experimental Section for details) as a representative example. The percent conversion versus irradiation time plots, along with the IR spectra of the monomer mixture before and after exposure,

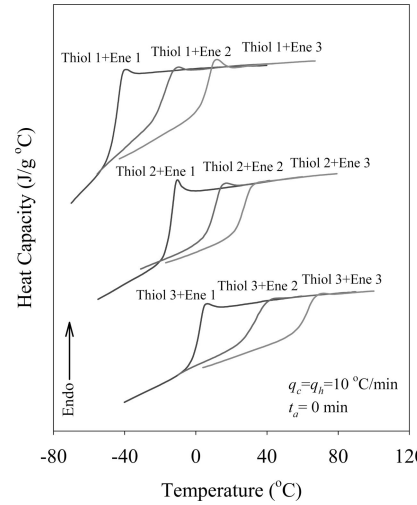

Figure 3. DSC thermograms of photopolymerized thiol−ene films (q_c = q_h = 10 °C/min, t_a = 0 min).

clearly illustrate essentially complete conversion even for the relatively low light intensity used in this real-time infrared analysis. From this representative example, which is consistent with an extensive literature as reported in the review reference,[17] it is clear that all of the samples in Figure 3 attained quantitative conversion. All samples used for the aging studies were prepared by exposing 10 times at 10 feet/min to the output of a Fusion D bulb with irradiance of 3.1 W/cm^2 followed by postcuring at 80 °C for 24 h. This ensures quantitative conversion for all samples prior to beginning the enthalpy relaxation measurements.

Upon closer evaluation of the results in Figure 3, it is apparent that the glass transition temperature is a function of network density (i.e., the linking or connecting density) and the bulkiness (rigidity) of the network components. For a given ene, the films made with Thiol 1 have the lowest glass transition temperature, consistent with the low functionality of Thiol 1. The glass transition temperature increased with increasing thiol functionality; i.e., the films made from the tetrafunctional thiol (Thiol 3)

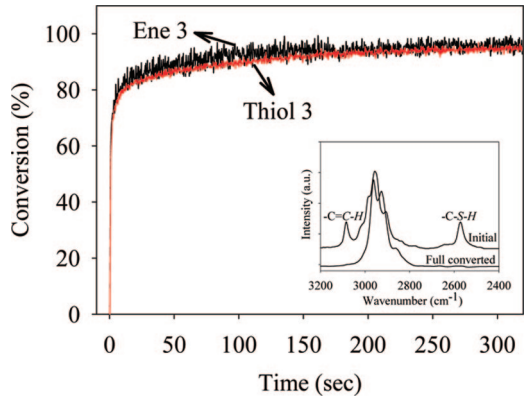

Figure 4. Conversion of −SH and −C═C− vs irradiation time for the Thiol 3 + Ene 3 system.

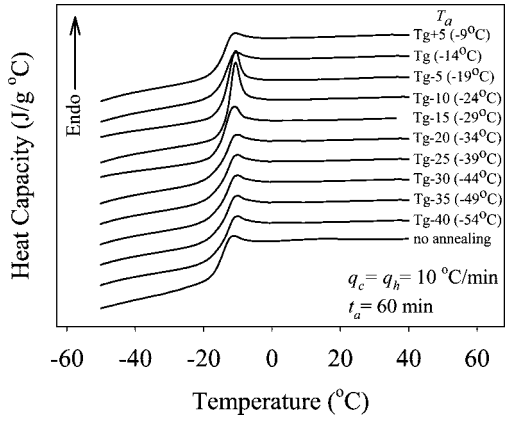

Figure 5. DSC heating scans a thiol−ene film (Thiol 2 + Ene 1) after annealing at different temperatures (t_a = 60 min, q_h = q_c = 10 °C/min).

had the highest glass transition temperatures for a given ene. Also, samples incorporating Ene 2 and Ene 3 with the rigid triazine rings have higher glass transition temperatures than those prepared using Ene 1. This is consistent with previous results for other thiol−ene networks.[17]

Thiol−ene films were annealed at specific temperatures (T_a = annealing temperature) every 5 °C from T_g + 10 to T_g − 50 °C for a time (60 min), t_a, to investigate the temperature dependency of enthalpy relaxation. Figure 5 shows DSC heating scans of a selected thiol−ene system (Thiol 2 + Ene 1) after annealing at different temperatures. A similar annealing process followed by DSC scans was performed for each of the thiol−ene samples. The resultant areas of the relaxed enthalpy peaks as a function of ΔT_a (T_g − T_a) for all of the thiol−ene systems are plotted in Figure 6. The plots in Figure 6 resemble asymmetric bell-shaped curves with the maxima located at about T_g − 10 °C. At temperatures well below T_g, i.e., (T_g − T_a) > 30 °C, the structural relaxation rate is slow as exemplified by longer characteristic relaxation times. Hence, during the 1 h annealing time, the relaxed enthalpy is small. As the annealing temperature increases, (T_g − T_a) becomes smaller, and the relaxation process becomes progressively faster. Thus, the relaxed enthalpy achieved during the 1 h annealing time increases. At annealing temperatures near the glass transition, the extent of relaxed enthalpy achieved in the 1 h annealing period will be limited not by the characteristic relaxation time, but rather the actual enthalpic departure from equilibrium at that temperature. Hence, the maximum in the relaxed enthalpy occurs at about T_g − 10 °C for each of the systems depicted in Figure 6. On the basis of the results presented in Figure 6, two molecular factors controlling the relaxed enthalpy maximum, the network density

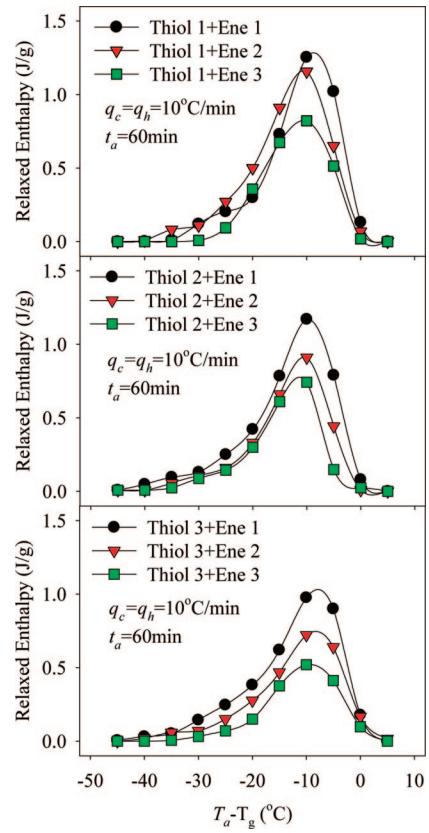

Figure 6. Temperature dependency and monomer structural effect on enthalpy relaxation of thiol−ene films (t_a = 60 min, q_h = q_c = 10 °C/min).

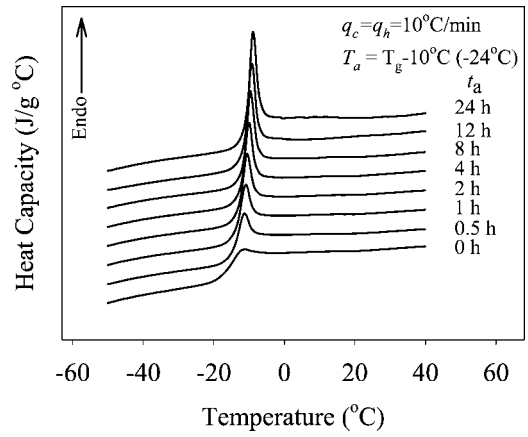

Figure 7. DSC heating scans of a thiol−ene film (Thiol 2 + Ene 1) after annealing for different annealing times (T_a = T_g − 10 °C, q_h = q_c = 10 °C/min).

and the bulkiness (rigidity) of network constituents, are considered. It is obvious from the results in Figure 6 that the relaxed enthalpy maximum decreases with an increase of either of these two network parameters. Specifically, the films made from monomer combinations having higher thiol functionalities (Thiol 3 > Thiol 2 > Thiol 1) and enes with more rigid structure (Ene 3 > Ene 2 > Ene 1) exhibit less enthalpy relaxation during the 1 h annealing period.

Figure 7 shows DSC heating scans for a representative system (Thiol 2 + Ene 1) after annealing for different time periods at T_g − 10 °C, the temperature where enthalpy relaxation exhibited a maximum during the isochronal analysis. The enthalpy relaxation peaks consistently increased with annealing time (t_a). The isothermal annealing results in Figure 7 for the Thiol 2 +

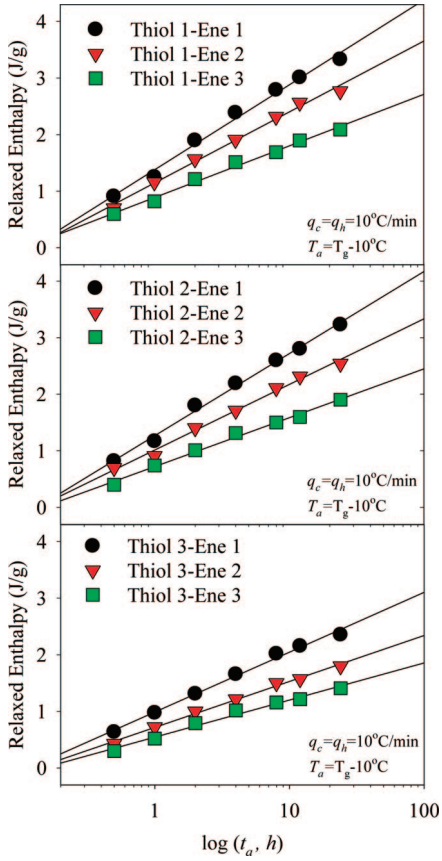

Figure 8. Relaxed enthalpy vs logarithmic annealing time of thiol−ene networks ($T_a = T_g - 10$ °C, $q_h = q_c = 10$ °C/min).

Ene 1 system, and equivalent results obtained for the other eight thiol−ene systems are plotted in Figure 8. A simple method for analyzing the general overall relaxation rate (β_H)[26−30] according to eq 2 can be applied to the plots in Figure 8.

$$\beta_H = \frac{d\delta_H}{d \log t_a} \tag{2}$$

It is clear that the β_H values obtained from the extent of enthalpy relaxation (δ_H) vs logarithmic annealing time (t_a) at T_a in Figure 8 decrease with the thiol functionality (network density) and ene bulkiness (rigidity) which, as already discussed, are molecular factors which influence the relaxation process. The low 24 h enthalpy relaxation values ($\Delta H_{24\,h}$) for the systems with the more rigid triazine ring structures might well have been expected from a literature reference which indicates that bulky groups, albeit on the side groups in linear polymers, also result in low enthalpy relaxation values.[9]

Additional evidence for the difference in the relaxation processes for the films produced from the nine thiol−ene combinations can be suggested by calculating ΔC_p at T_g for the original DSC scans in Figure 3. According to the definition of fictive temperature and assuming that equilibrium conditions ($T_f = T_a$ at $t_a = \infty$) are attained, the ultimate enthalpy relaxation values (ΔH_∞) at a given annealing temperature (T_a) can be approximated by the product of ΔC_p at T_g and ΔT_a ($T_g - T_a$).[1,2]

$$\Delta H_\infty(T_a) \approx \Delta C_p(T_g)\Delta T_a \tag{3}$$

The resultant values for ΔC_p at T_g and $\Delta C_p \Delta T_a$ in Table 1, like the results for $\Delta H_{24\,h}$, decrease as the thiol functionality increases from 2 to 4 and the ene rigidity increases. This results from the relationship between the amount of excess enthalpy and ΔC_p at T_g.

Table 1. Extents of Enthalpy Relaxation at 24 h ($\Delta H_{24\,h}$), Overall Relaxation Rates (β_H), Heat Capacities at T_g (ΔC_p), and Assumed Maximum Enthalpy Relaxation ($\Delta C_p \Delta T_a$) for Photopolymerized Thiol−Ene Networks

sample	$\Delta H_{24\,h}$ (J/g)	β_H (J/g per decade)	ΔC_p (J/(g °C))	$\Delta C_p \Delta T_a$[a] (J/g)
Thiol 1 + Ene 1	3.331	1.501	0.5624	5.624
Thiol 1 + Ene 2	2.600	1.254	0.5251	5.251
Thiol 1 + Ene 3	2.089	0.912	0.3739	3.739
Thiol 2 + Ene 1	3.231	1.451	0.4985	4.985
Thiol 2 + Ene 2	2.103	1.160	0.3633	3.633
Thiol 2 + Ene 3	1.903	0.863	0.3360	3.360
Thiol 3 + Ene 1	2.356	1.058	0.3847	3.847
Thiol 3 + Ene 2	1.798	0.813	0.3079	3.079
Thiol 3 + Ene 3	1.409	0.656	0.2514	2.514

[a] $\Delta T_a = T_g - T_a = 10$ °C.

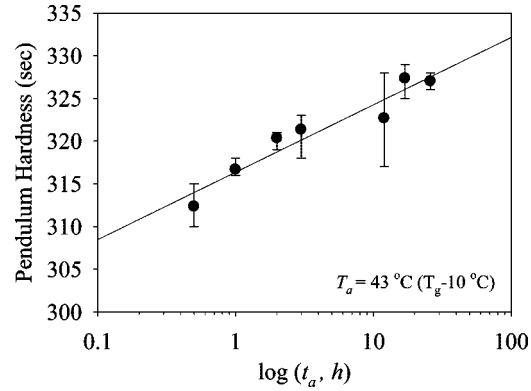

Figure 9. Persoz pendulum hardness for Thiol 3−Ene 3 as a function of annealing time (t_a).

Finally, to demonstrate the effect of annealing on thiol−ene film hardness, Thiol 3 + Ene 3 films coated on glass plates were isothermally annealed at 43 °C (T_g − 10 °C) and, after each annealing time period, cooled to room temperature (20 °C) for measurement. A linear relationship between the Persoz hardness and the logarithm of the annealing time clearly illustrates the effect of sub-T_g aging on physical property changes.

Conclusions

Photopolymerized thiol−ene films were evaluated in terms of enthalpy relaxation. Maximum enthalpy relaxation was observed at T_g − 10 °C for all thiol−ene films investigated. The extent of enthalpy relaxation after 24 h of annealing ($\Delta H_{24\,h}$) and the overall relaxation rate (β_H) determined by the slope of the extent of enthalpy relaxation (δ_H) vs the logarithm of the annealing time (t_a) plot decreased with ene rigidity and the functionality of the thiols used to fabricate the thiol−ene network. The assumed maximum enthalpy relaxation (ΔH_∞) at the annealing temperature as well as the heat capacity difference (ΔC_p) at T_g also showed that the relaxation process is affected by the molecular structural features, i.e., rigidity and functionality. Physical property changes monitored by Persoz hardness increased as a function of annealing time coincident with the enthalpy relaxation. Considering that thiol−ene networks are used at temperatures below T_g, the effect of sub-T_g aging on other physical and mechanical properties is critical to evaluate.

Acknowledgment. We acknowledge Perstorp, Bruno Bock, and Ciba Specialty Chemicals for materials and Fusion UV Systems for the light source.

References and Notes

(1) Hutchinson, J. M.; Kumar, P. *Thermochim. Acta* **2002**, *391*, 197.
(2) Huang, D.; Yang, Y.; Zhuang, G.; Li, B. *Macromolecules* **1999**, *32*, 6675.

(3) Andreozzi, L.; Faetti, M.; Giordano, M.; Zulli, F. *Macromolecules* **2005**, *38*, 6056.
(4) Andreozzi, L.; Faetti, M.; Giordano, M.; Palazzuoli, D. *J. Non-Cryst. Solids* **2003**, *332*, 229.
(5) Privalko, V.; Demchenko, S. S.; Lipatov, Y. S. *Macromolecules* **1986**, *19*, 901.
(6) Aras, L.; Richardson, M. J. *Polym. Commun.* **1985**, *26*, 77.
(7) Tsitsilianis, C.; Mylonas, I. *Makromol. Chem., Rapid Commun.* **1992**, *13*, 207.
(8) Huang, D.; Yang, Y.; Zhuang, G.; Li, B. *Macromolecules* **2000**, *33*, 461.
(9) McGonigle, E. A.; Cowie, J. M. G.; Arrighi, V.; Pethrick, R. A. *J. Mater. Sci.* **2005**, *40*, 1869.
(10) Roe, R. J.; O′Reilly, J. M. *Structure, Relaxation, and Physical Aging of Glassy Polymers*; Materials Research Society: Pittsburgh, 1991.
(11) Kalakkunnath, S.; Kalika, D. S.; Lin, H.; Freeman, B. D. *Macromolecules* **2005**, *38*, 9679.
(12) Lin, Y. G.; Sauterreau, H.; Pascault, J. P. *J. Appl. Polym. Sci.* **1986**, *32*, 4595.
(13) Lee, A.; McKenna, G. B. *Polymer* **1988**, *29*, 1812.
(14) Plazek, D. J.; Frund, Z. N., Jr. *J. Polym. Sci., Part B: Polym. Phys.* **1990**, *28*, 431.
(15) Calventus, Y.; Montserrat, S.; Hutchinson, J. M. *Polymer* **2001**, *42*, 7081.
(16) Cortes, P.; Montserrat, S.; Hutchinson, J. M. *J. Appl. Polym. Sci.* **1997**, *63*, 17.
(17) Hoyle, C. E.; Lee, T. Y.; Roper, T. *J. Polym. Sci., Part A: Polym. Chem.* **2004***42*, 5301.
(18) Roper, T. M.; Rhudy, K. L.; Chandler, C. M.; Hoyle, C. E.; Guymon, C. A. *RadTech NA Tech. Conf. Proc.* **2002**, 697.
(19) Roper, T. M.; Guymon, C. A.; Hoyle, C. E. *Polymer* **2004**, *45*, 2921.
(20) Lub, J.; Broer, D. J.; Allan, J. F. *Mol. Cryst. Liq. Cryst. Sci. Technol., Sect. A* **1999**, *332*, 2769.
(21) Toh, H. K.; Chen, F.; Kok, C. M. U.S. Patent 6,172,140, **2001**.
(22) Cerrada, M. L.; McKenna, G. B. *Macromolecules* **2000**, *33*, 3065.
(23) Roe, R.-J.; Millman, G. M. *Polym. Eng. Sci.* **1983**, *23*, 318.
(24) Montserrat, S.; Calventus, Y.; Hutchinson, J. M. *Prog. Org. Coat.* **2006**, *35*, 42.
(25) Pellerin, C.; Pelletier, I.; Pezolet, M.; Prud'homme, R. R. *Macromolecules* **2003**, *36*, 153.
(26) Hutchinson, J. M. *Prog. Polym. Sci.* **1995**, *20*, 703.
(27) Pan, P.; Zhu, B.; Inoue, Y. *Macromolecules* **2007**, *40*, 9664.
(28) Ju, H.; Nutt, S. *Macromolecules* **2003**, *36*, 4010.
(29) Struik, L. C. E. *Polymer* **1987**, *28*, 1869.
(30) Struik, L. C. E. *Physical Aging in Amorphous Polymers and Other Materials*; Elsevier Publishing Co.: New York, 1978.

MA800863N